The Spectral p–n Junction Model for Tandem Solar-Cell Design

MATTHIAS E. NELL, MEMBER, IEEE, AND ALLEN M. BARNETT, SENIOR MEMBER, IEEE

Abstract—**Tandem solar cells can have significantly higher efficiencies than single-junction solar cells because they convert a larger fraction of the incident solar spectrum to electricity. For the design of tandem solar cells the spectral p–n junction model is proposed. It is based on tabulated standard spectra, on the fit of experimentally achieved open-circuit voltages, and assumes a quantum efficiency of unity. By consistent treatment of the energy gap in the diode equation, the model can be quantitatively applied to all tandem solar-cell systems. The special form and use of the reverse saturation current density is discussed in detail. The spectral p–n junction model is rigorously applied based on accepted standard spectra. The tandem solar-cell performance limits based on the model are calculated. A quantitative expression for the increase in efficiency under concentration is derived.**

Choosing materials with optimum bandgaps, a two-solar-cell two-terminal tandem system can achieve a theoretical maximum efficiency of 38.2-percent (*AM*1.5 global). A two-solar-cell four-terminal tandem system can have a maximum efficiency of 39.1 percent at the same spectrum. This four-terminal system allows more freedom in choosing the most efficient bandgap combinations. Assuming realistic losses, a configuration consisting of a Si solar cell on the bottom and a solar cell with a bandgap, E_g = 1.85 eV on the top, a maximum efficiency of 32.1 percent (*AM*1.5 global) can be predicted. Increased efficiency can be obtained from a three-solar-cell six-terminal tandem system. With an optimum bandgap combination the theoretical maximum efficiency is 44.5 percent (*AM*1.5 global) for the three-solar-cell system.

The limits predicted by the model are discussed for tabulated standard spectra. The highest achievable efficiency is 57.3 percent (*AM*1.5 global) without concentration of the incident light. The increase in efficiency under concentration is evaluated, and it is found that the relative change of the efficiency at any concentration X is linear with ln (X).

List of Symbols

A	Diode ideality factor.
C	Constant.
c	Velocity of light.
D_n, D_p	Diffusion constant for electrons, holes.
E_g	Bandgap.
e	Electric charge.
η	Efficiency.
F	Photon flux.
H'	Thickness of p-region.
h	Planck's constant.
I	Irradiance.
J	Current density.
J_{sc}	Short-circuit current density.
J_0	Reverse saturation current density.
k	Boltzmann's constant.
L_n, L_p	Diffusion length for electrons, holes.
λ	Wavelength.
m_e, m_h	Effective mass of electron, hole.
N_c, N_v	Effective density of states in conduction, valence band.
N_d, N_a	Doping density for n-, p-region.
n_i	Intrinsic carrier concentration.
P	Power.
P_m	Power of the maximum power point.
P_s	Total incident solar power.
S_p, S_n	Surface recombination velocity for minority holes, electrons.
T	Temperature.
V	Voltage.
V_{oc}	Open-circuit voltage.
V_m	Voltage of the maximum power point.
X	Concentration ratio of a concentrator system.
x	Phosphorus fraction in $GaAs_{1-x}P_x$.
x_j	Thickness of n-region.

Manuscript received September 16, 1985; revised July 1, 1986. This work was supported in part by the United States Air Force, Wright Aero Propulsion Laboratory.

M. E. Nell was with the Department of Electrical Engineering, University of Delaware, Newark, DE 19716. He is now with the Institut für Werkstoffe der Elektrotechnik, Technische Universität Berlin, Jebensstrasse 1, 1000 Berlin 12, Germany.

A. M. Barnett is with the Department of Electrical Engineering, University of Delaware, Newark, DE 19716.

IEEE Log Number 8611228.

I. Introduction

SINGLE-JUNCTION solar cells are limited in efficiency. The maximum theoretical limit depends on the incident spectrum. It is 28.3 percent for *AM*1.5 global and smaller for the other standard spectra. Tandem solar cells can have higher efficiency. For the two-solar-cell tandem system the theoretical maximum at *AM*1.5 global is 39.1 percent.

The idea of converting different parts of the incident solar spectrum by different solar cells has been considered since 1955 [1], [2]. Recently theoretical and experimental studies of tandem or cascade solar cells have been reviewed by Loferski [3], multijunction concentrator solar cells by Mitchell [4] and Hutchby *et al.* [5]. The design of a two-junction monolithic cascade solar cell has been discussed by Lamorte *et al.* [6], [7]. Fan *et al.* [8] discuss the optimal design of high-efficiency tandem solar cells. The maximum-efficiency solar-cell structure was determined by Pauwels *et al.* [9]. Riordan *et al.* [10] calculate the dependence of the efficiency on air mass and atmo-

spheric conditions for a single-junction solar cell and two- and three-solar-cell tandem systems.

The best reported efficiency for a filter-reflector configuration is 28.5 percent under concentration [11] and 21.3 percent at 130 × *AM*3 for a monolithic two-bandgap solar cell [12]. As the interest in high-efficiency tandem solar cells increases, a consistent detailed design methodology is needed for comparison of various designs.

One part is the determination of the bandgap combination which will provide maximum performance. The spectral p–n junction model is proposed for this design step. It is based on tabulated spectra, on the fit of experimentally achieved open-circuit voltages, and assumes a quantum efficiency of unity. It is able to generate data to determine that tandem solar-cell bandgap combination for maximum efficiency.

The model can also be used to predict realistic tandem solar-cell performance by assuming losses. For the detailed design of solar cells in the tandem structure the absorption coefficient has to be taken into account to determine the dimensions and doping of the solar cells.

II. Tandem Solar Cells for High Efficiency

The analysis of single-junction solar-cell performance as done by Wolf [13] for *AM*0 shows that only a small part of the available theoretical maximum energy is converted to usable power. The two major losses come from photons that are not absorbed (24.0 percent), because their energy is lower than the energy gap, and photons, whose energy is greater than the gap (32.5 percent), but do not create more than one electron–hole pair. For higher energy photons the energy is dissipated in the form of heat.

To convert more of the incident power lost by unconverted photon energy in a single-junction solar cell (24.0 percent + 32.5 percent = 56.5 percent), systems with more than one energy gap have to be used. By splitting the spectrum in parts and directing each to a solar cell with a suitable bandgap, the efficiency of the energy conversion can be increased [1], [2]. To realize this suggestion two single junctions can be put in tandem, called "tandem" or "multicolor" solar cells. Another idea is directing parts of the solar spectrum by semi-transparent reflectors to materials with different bandgaps. This solar-cell configuration is called "filter-reflectors."

The most suitable device for tandem solar cells is a concentrator configuration. It offers advantages because with its small optical focus the size and cost of the energy converter can be reduced. The concentrator configuration focuses multiple times the intensity of the sun on the solar cell. Therefore the solar cells are more efficient, provide higher power, and due to the small size can be less expensive per unit of energy converted.

For a two-solar-cell tandem system, three different wiring configurations have been described. The device might have two, three, or four terminals. For a serial two-terminal tandem system the short-circuit currents of lower and upper solar cell have to be matched for high efficiency. The calculations show that this constraint leads to lower maximum efficiencies and a greater limitation in the choice of bandgaps. Two different connections for a two-solar-cell three-terminal tandem system are proposed [14]. Both the complementary three-terminal device [15] and the setup with an additional single junction [8] are difficult to connect and require the match of currents. The parallel-connected two-solar cell four-terminal configuration has advantages. It is technically simpler, has more flexibility in the choice of bandgaps, no constraints related to the currents, and offers the opportunity to supply power for two different loads.

III. The Data for the Solar Spectra

For terrestrial solar simulation and solar-cell efficiency measurements, Matson *et al.* [16] have proposed modeled spectra, which are accepted as standards. The direct normal irradiance standard at *AM*1.5 (*AM*1.5 direct) represents the spectrum of the sunlight on earth, where the light is incident directly without any contribution from diffuse rays. Because of its direct character this spectrum is preferred for the calculation of terrestrial concentrator solar-cell system efficiencies. The total incident power density is 75.219 mW/cm^2.

The global spectral irradiance standard at *AM*1.5 (*AM*1.5 global) is also computer generated by a rigorous radiative transfer code to represent a solar spectrum incident on the earth. It includes direct and diffuse rays from the sun. The total incident power density is 96.971 mW/cm^2. New spectra to improve *AM*1.5 direct and *AM*1.5 global are being developed [17].

Calculations for situations in the outer space can be done with the solar spectral-irradiance standard curve (*AM*0) [18], which was generated by measurements from aircraft. The solar constant, the total amount of power incident from the sun at unit area in the orbit, was determined to be 135.3 mW/cm^2.

IV. The Spectral p–n Junction Model

The spectral p–n junction model is proposed to evaluate the theoretical maximum efficiency of solar cells and to provide data for the design of tandem solar cells. The generated current density dependent on the bandgap is calculated directly from spectral data. The open-circuit voltage is determined by the calculated short-circuit current density, the reverse saturation current density is dependent on the bandgap and the temperature. The fill factor is determined with the calculated maximum power point. Based on the bandgap and the available current density, the power generated by each of the tandem solar cells can be computed. Further, the model can be used to calculate the efficiency for tandem solar-cell systems under concentrated light.

The short-circuit current density J_{sc} was calculated directly from the irradiance data. These data are integrated by rectangle rule integration. The photon flux F is calculated from the irradiance I and the wavelength λ.

$$F = \frac{\lambda \cdot I}{h \cdot c}. \tag{1}$$

The current density at quantum efficiency of unity, when every incident photon creates an electron, can be found by multiplying the photon flux with the electric charge e.

$$J_{sc} = e \cdot F. \tag{2}$$

The optical absorption is considered to be complete for energies higher then the bandgap. For lower energies no absorption takes place, no carriers are generated. For smaller quantum efficiencies a model for the optical absorption has to be assumed, respectively.

The reverse saturation current density J_0 of a p–n junction n on p solar cell is given by (3) [19]. It is strongly determined by the proportionality to n_i^2.

$$J_0 = e \cdot \frac{n_i^2}{N_d} \cdot \frac{D_p}{L_p} \cdot \frac{\frac{S_p \cdot L_p}{D_p} \cdot \cosh\frac{x_j}{L_p} + \sinh\frac{x_j}{L_p}}{\frac{S_p \cdot L_p}{D_p} \cdot \sinh\frac{x_j}{L_p} + \cosh\frac{x_j}{L_p}} + e \cdot \frac{n_i^2}{N_a} \cdot \frac{D_n}{L_n} \cdot \frac{\frac{S_n \cdot L_n}{D_n} \cdot \cosh\frac{H'}{L_n} + \sinh\frac{H'}{L_n}}{\frac{S_n \cdot L_n}{D_n} \cdot \sinh\frac{H'}{L_n} + \cosh\frac{H'}{L_n}}. \tag{3}$$

The intrinsic carrier concentration n_i can be represented by (4) and (5).

$$n_i^2 = N_c \cdot N_v \cdot \exp\left(-\frac{E_g}{k \cdot T}\right) \tag{4}$$

$$= 4 \cdot \left(\frac{2 \cdot \pi \cdot k \cdot T}{h^2}\right)^3 \cdot m_e^{*3/2} \cdot m_h^{*3/2} \cdot \exp\left(-\frac{E_g}{k \cdot T}\right). \tag{5}$$

The spectral p–n junction model uses (6) to represent the reverse-saturation current density over the entire range of desired bandgaps.

$$J_0 = C \cdot T^3 \cdot \exp\left(-\frac{E_g}{k \cdot T}\right) \tag{6}$$

$$= 4 \cdot \left(\frac{2 \cdot \pi \cdot k}{h^2}\right)^3 \cdot m_e^{*3/2} \cdot m_h^{*3/2} \cdot e \times \left(\frac{1}{N_d} \cdot \frac{D_p}{L_p} \cdot \frac{\frac{S_p \cdot L_p}{D_p} \cdot \cosh\frac{x_j}{L_p} + \sinh\frac{x_j}{L_p}}{\frac{S_p \cdot L_p}{D_p} \cdot \sinh\frac{x_j}{L_p} + \cosh\frac{x_j}{L_p}} + \frac{1}{N_a} \cdot \frac{D_n}{L_n} \cdot \frac{\frac{S_n \cdot L_n}{D_n} \cdot \cosh\frac{H'}{L_n} + \sinh\frac{H'}{L_n}}{\frac{S_n \cdot L_n}{D_n} \cdot \sinh\frac{H'}{L_n} + \cosh\frac{H'}{L_n}}\right). \tag{7}$$

TABLE I
COMPARISON OF EXPERIMENTALLY ACHIEVED OPEN-CIRCUIT VOLTAGES AND THE MODEL

Material	Energy Gap Eg (eV)	Spectrum	Temp. T (°C)	Experiment Voc (V)	Ref.	Model Voc (V)
Si	1.12	AM0	25	0.694	[17]	0.709
GaAs	1.424	AM1.5 global	27	1.04	[18]	0.996

In that way the dimensions, the doping, and the material parameters of a solar cell are combined in this one constant, C. In the model, the variable (see (7)) is always kept constant. The only solar-cell parameters important for the model calculations are the temperature and bandgap.

Green gives a model for the reverse-saturation current density derived from Shockley's expression [20]. The product $C \cdot T^3$ is replaced by a constant $1.5 \cdot 10^8$ mA/cm^2 [21]. Loferski discusses cases where $C \cdot T^3$ is equal to 1 mA/cm^2 and $1.44 \cdot 10^8$ mA/cm^2. In a third model he introduces $C \cdot T^3$ dependent on the diffusion length [22].

It is clear that the optimized design includes a minimized value for C. It is premature to conclude that there is a single value that is applicable to all materials. Typically a value is determined by matching experimental results.

To base the model on realistic data, Fan chose C by a fit of experimentally achieved open-circuit voltages [8]. The value was 50 mA/cm$^2 \cdot$ K^3, based on the open-circuit voltage for Si of 0.65 V and for GaAs of 0.98 V. Recent highest reported open-circuit voltages are for Si 0.694 V (*AM*0, 25°C) [23] and for GaAs 1.04 V (*AM*1) [24]. Assuming similarity of the spectra, *AM*1.5 global instead of *AM*1 was used for the model fit. The tabulation in Table I shows the comparison between experimental and calculated values for $C = 17.90$ mA/cm$^2 \cdot$ K^3, the arithmetic average of the best fit for Si and GaAs.

Although the constant C affects performance logarithmically, reasonable variations around the value 17.90 mA/cm$^2 \cdot$ K^3 will only have a modest effect on the overall system efficiency. For example, if C is reduced by a factor of 2 to 8.95 mA/cm$^2 \cdot$ K^3, the open-circuit voltage of the top solar cell would be increased by 1.2 percent and the bottom solar cell by 2.5 percent. The change in fill factor would be negligible and there would be no change in short circuit-current density. Accordingly the most efficient two-solar-cell tandem system described by this model would increase by 1.9 percent from 39.11 to 39.85 percent. If the value of C was chosen the optimum fit for GaAs, 3.26 mA/cm$^2 \cdot$ K^3 (a reduction by a factor of 5.5), the best two-solar-cell tandem efficiency would increase by 4.7 to 40.93 percent. The open-circuit voltage of GaAs is very close to the theoretical maximum. For Si a major breakthrough has to be achieved to solve the problems of surface recombination and increase the open-circuit voltage. Therefore the choice of C in this work is considered to be realistic, and a little conservative. A more accurate

value of C will require the complete development of additional materials for solar cells.

$$V_{oc} = \frac{A \cdot k \cdot T}{e} \cdot \ln\left(\frac{J_{sc}}{J_0} + 1\right). \quad (8)$$

With (8) the open-circuit voltage can be calculated dependent on the bandgap for the standard spectra. The diode ideality factor A is assumed to be 1 in this entire paper and therefore not mentioned again. The open-circuit voltage shows an insignificant dependence on the different spectra. Only for photon energies higher than 3.5 eV will the voltage for the various spectra differ by a maximum of 5.4 percent. According to (8), the voltage will increase, if the light intensity, e.g., the photon flux, is raised. But there is only a small difference in V_{oc}, if spectrum *AM*0 or *AM*1.5 direct is used.

V. Efficiencies of Single-Junction Solar Cells

The reverse saturation current density is modeled to enable the calculation of the power and efficiency of a single-junction solar cell. These data can help to select a material with a bandgap, which will lead to a solar cell operating at the maximum achievable efficiency.

To determine the maximum power point $P_{\max}$ the voltage–current (density) characteristic for a single-junction solar cell has to be considered.

$$J = J_{sc} + J_0 \cdot (e^{e \cdot V/kT} - 1). \quad (9)$$

The maximum power point, i.e., the maximum of the power P dependent on the voltage (10) has to be found.

$$P = V \cdot J = V \cdot (-J_{sc} + J_0 \cdot (e^{e \cdot V/kT} - 1)). \quad (10)$$

This point can be calculated by setting the derivative equal to zero as shown in (11) [25].

$$\left(\frac{dP}{dV}\right)_{V_m} = -J_{sc} - J_0 + J_0 \cdot \left(1 + \frac{e \cdot V_m}{k \cdot T}\right) \cdot e^{e \cdot V_m/k \cdot T} = 0. \quad (11)$$

The efficiency is determined normalizing the power by the total incident power of the spectrum.

Fig. 1 shows the efficiencies for a single-junction solar cell as a function of the bandgap based on the different spectra. The *AM*0 spectrum represents the highest incident power, but the calculated efficiency is less than that for the spectra *AM*1.5 global and *AM*1.5 direct. This normalizing constant results in lower efficiencies for *AM*0, but high power, because the single junction will not convert to electricity infrared photons, which are of less than bandgap energy.

The band energies with the highest efficiency are drawn in Fig. 1. From these data it can be concluded that GaAs with a bandgap of 1.424 eV is the material with the optimum bandgap.

Fig. 1 shows different qualitative and quantitative results than those described by Prince [26]. He plots the power density versus bandgap as a smooth bow curve with a maximum at 1.25 eV. Loferski calculates the efficiency versus bandgap energy varying the solar altitude and the effect of water vapor absorption [22]. Maxima from 1.3 to 1.6 eV are shown. For the results described here, the spectral information is taken directly from the previous spectra, which represent standards accepted by ASTM.

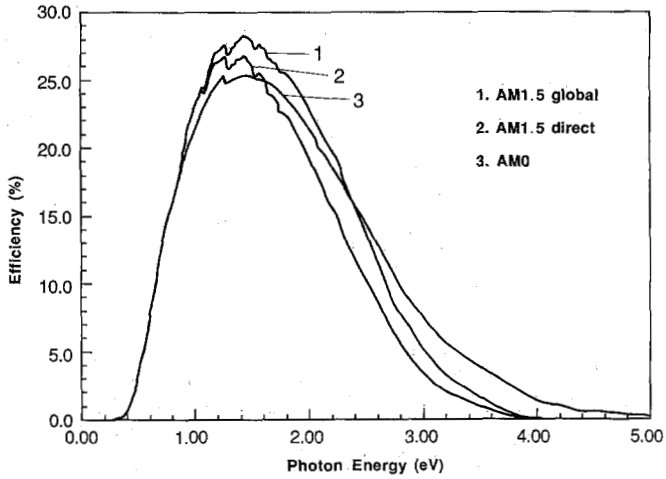

Fig. 1. Single-junction solar-cell efficiencies for the standard spectra.

The efficiency dependent on the bandgap for the extraterrestrial spectrum shows a spike at 1.24 eV, which can be related to a sudden drop in J_{sc} going to higher energies. The spectra for *AM*1.5 have a lot of structure between 1 and 2 eV. This results in structured maximum-efficiency curves. The local maxima and minima are due to atmospheric absorption, e.g., by water vapor (H_2O), oxygen (O_2), or carbon dioxide (CO_2). Therefore an exact choice or accurate process control of the bandgap will be required to operate at the theoretical maximum efficiency.

VI. Efficiencies of Two-Solar-Cell Tandem Systems

The simplest tandem system consists of two solar cells. For the design of the top and bottom solar cell the bandgaps of the materials selected must be known. The spectral p–n junction model can provide data to determine the bandgap combination, which will yield the highest possible efficiency.

The calculations are based directly on the available spectral data sets. Starting with the irradiance data point at the highest energy, the performance was calculated for the upper solar cell. The remaining part of the spectrum was taken to calculate the performance of the lower solar cell. The highest added efficiencies of the top and the bottom solar cells were drawn dependent on the different spectra.

Figs. 2, 3, and 4 show the theoretical maximum efficiencies of two-solar-cell two-terminal tandem systems for the spectra *AM*1.5 global, *AM*1.5 direct, and *AM*0. Areas of efficiency within a certain limit are marked. The calculated regions are small and close. This indicates that

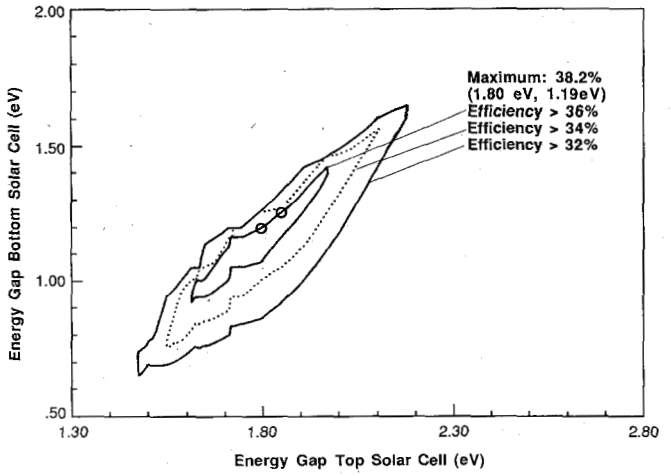

Fig. 2. Two-solar-cell two-terminal tandem system efficiencies for the spectrum *AM*1.5 global.

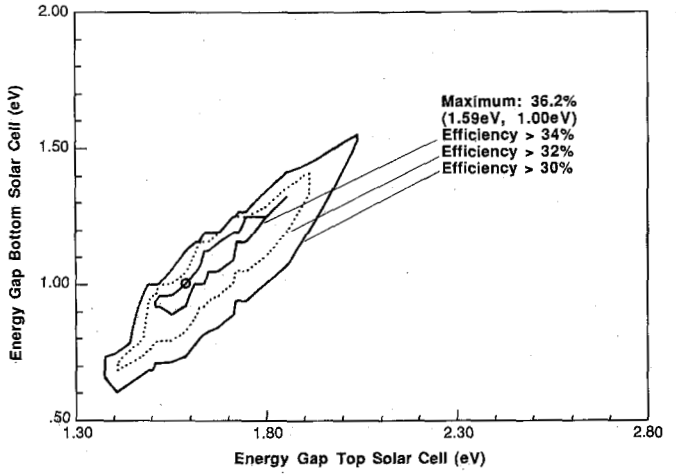

Fig. 3. Two-solar-cell two-terminal tandem system efficiencies for the spectrum *AM*1.5 direct.

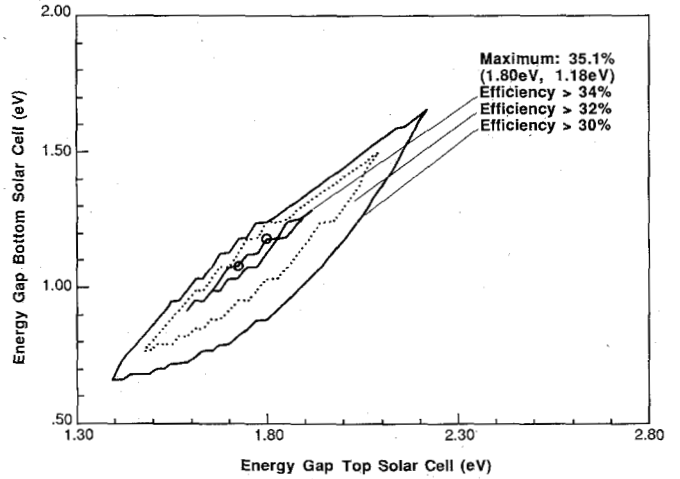

Fig. 4. Two-solar-cell two-terminal tandem system efficiencies for the spectrum *AM*0.

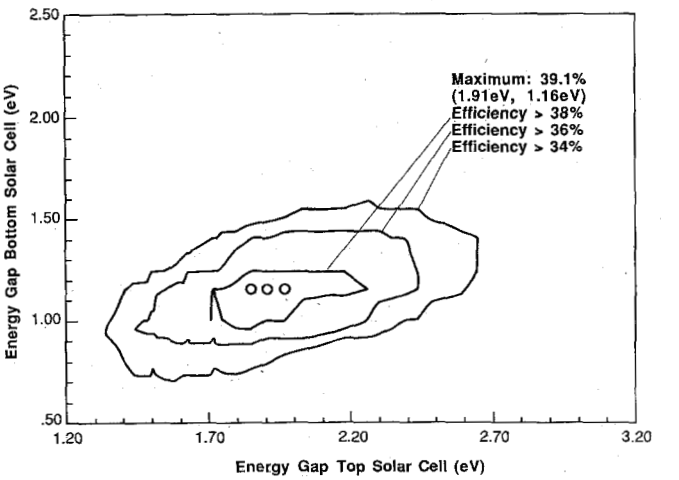

Fig. 5. Two-solar-cell four-terminal tandem system efficiencies for the spectrum *AM*1.5 global.

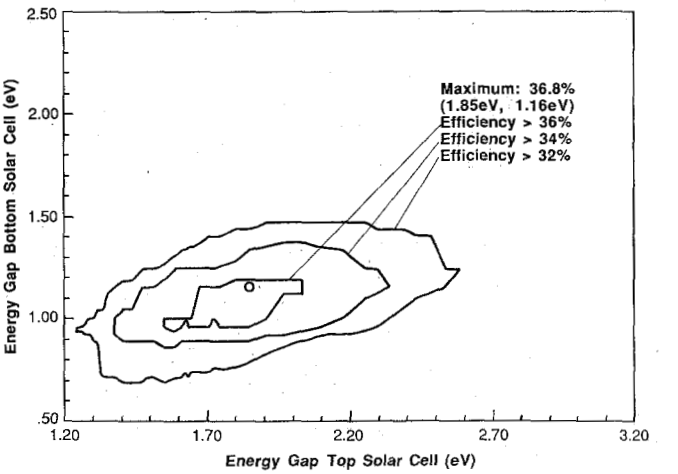

Fig. 6. Two-solar-cell four-terminal tandem system efficiencies for the spectrum *AM*1.5 direct.

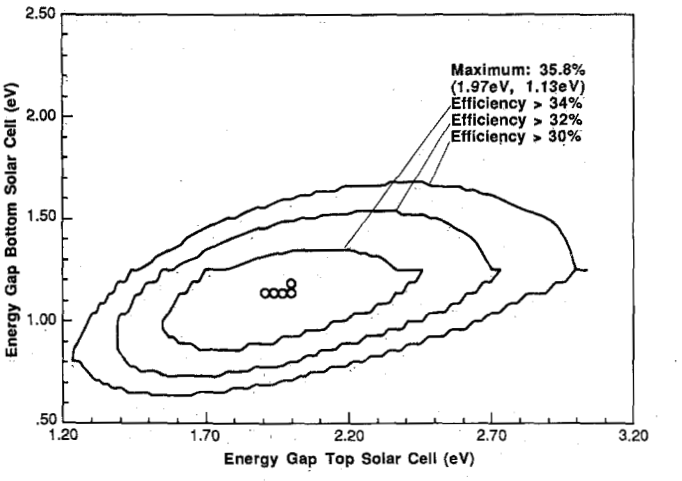

Fig. 7. Two-solar-cell four-terminal tandem system efficiencies for the spectrum *AM*0.

there is only a limited choice for the most efficient bandgap combinations.

The maximum efficiencies for two-solar-cell four-terminal tandem systems are drawn in Figs. 5, 6, and 7. The obtained area limits have a round shape. For a given bottom solar cell there is a wide range of bandgaps for the top solar cell available. Therefore this configuration offers more freedom for the choice of bandgaps than the two-

TABLE II
MAXIMUM SINGLE-JUNCTION, TWO- AND THREE-SOLAR-CELL, TWO-, FOUR-, AND SIX-TERMINAL TANDEM SYSTEM EFFICIENCIES DEPENDENT ON THE BANDGAP FOR THE STANDARD SPECTRA

Spectrum	Solar Cell Band Gap (eV)			Max. Effic. (%)
	Single Junction			
AM1.5 global	1.41			28.28
AM1.5 direct	1.41			26.76
AM0	1.44			25.18
	2 Solar Cell Tandem System			
	Top	Bottom		
AM1.5 global	1.91	1.16		39.11
AM1.5 direct	1.85	1.16		36.83
AM0	1.97	1.13		35.79
	3 Solar Cell Tandem System			
	Top	Middle	Bottom	
AM1.5 global	2.25	1.55	1.00	44.45
AM1.5 direct	2.03	1.41	0.96	42.16
AM0	2.30	1.55	0.99	40.89

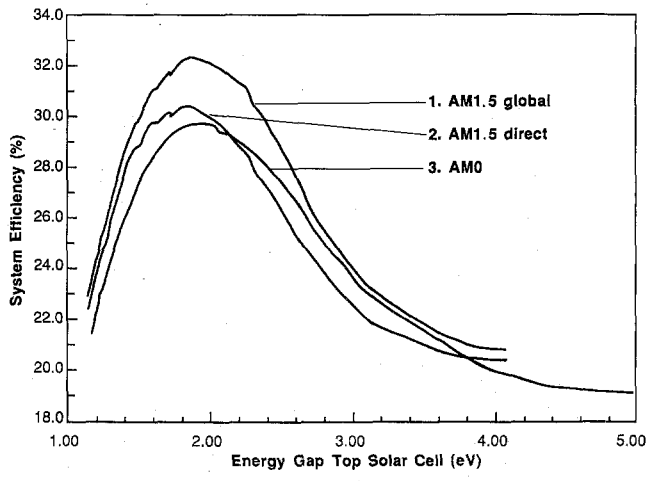

Fig. 8. Two-solar cell four-terminal tandem solar-cell efficiencies including losses with silicon bottom solar cell (E_g = 1.1273 eV) for the standard spectra dependent on the bandgap of the top solar cell.

terminal case. The graphs represent a structure, which is related to the irradiance distribution. The maximum efficiency for *AM0* covers a larger range of bandgaps, while the *AM*1.5 spectra have a more distinct maximum. Also this can be attributed to the original spectrum, which is very smooth in the range of interest with a flat maximum for *AM0*, but strongly structured for *AM*1.5. The numerical values in Table II are taken from the graphs to compare the performance. Table II also shows the maximum performance for the three-solar-cell six-terminal system.

For the rest of this work only tandem configurations will be considered, where each solar cell is connected separately. The advantages are the wide range of available bandgaps for maximum efficiency and the higher predicted system efficiencies.

VII. REALISTIC TWO-SOLAR-CELL TANDEM SYSTEM PERFORMANCE

Particularly the interest in tandem solar cells is directed towards a structure consisting of a top solar cell made from ternary III–V semiconductors, e.g., $GaAs_{1-x}P_x$ [27], [28], and a silicon bottom solar cell. The bandgap of silicon is very close to the bandgap of the bottom solar cell for the theoretical maximum-efficiency tandem system. The silicon solar cell is the most developed solar cell, and it is available in the market in many forms, which gives flexibility for building the tandem solar-cell system using current technology.

Fig. 8 shows the result of model calculations for a two-solar-cell tandem system including losses with a bottom solar cell having a bandgap of 1.1273 eV to represent silicon. This bandgap value for silicon was chosen to permit the spectral p–n junction model to be based directly on the spectral irradiance standards. To test the sensitivity of this bandgap choice, calculations with spectra extended by the irradiance at the wavelength for a silicon bandgap (1.12 eV = 1.1071 μm) were made. These calculations in general show a very small change in efficiency qualitatively and quantitatively for single junctions as well as for tandem solar cells. In particular, the tandem solar-cell efficiency drops. In the highest efficient two-solar-cell four-terminal tandem system, the bottom solar-cell efficiency changes from 11.30 to 11.18 percent (*AM*1.5 global). The top solar-cell efficiency stays unchanged. That is caused by different integration intervals for the extended spectra. Therefore the standard spectra used in this paper have not been changed to better match the bandgap of silicon.

To estimate realistic tandem solar-cell performance the efficiency calculations were carried out with added optical losses, which reduce the short-circuit current, and electrical losses, which reduce the generated power, for the top and the bottom solar cell. In particular, it was accounted for after Barnett *et al.* [29], Gee [30], and McNeely *et al.* [31]:

1) Losses for the Top Solar Cell
   a) Optical Losses
      surface reflection, anti-reflection-coating 2.6 percent
      grid shading 4.0 percent
      absorption 2.0 percent
      recombination 6.2 percent
   b) Electrical Losses
      series resistance losses 2.0 percent
2) Losses for the Bottom Solar Cell
   a) Optical Losses
      interface reflection 2.0 percent
      surface reflection, anti-reflection-coating 2.0 percent
      absorption 9.0 percent
      recombination 6.2 percent
   b) Electrical Losses
      series resistance losses 2.0 percent

To calculate an overall loss for each solar cell the given values have to be converted to fractions and multiplied because the losses occur one after the other. For the top

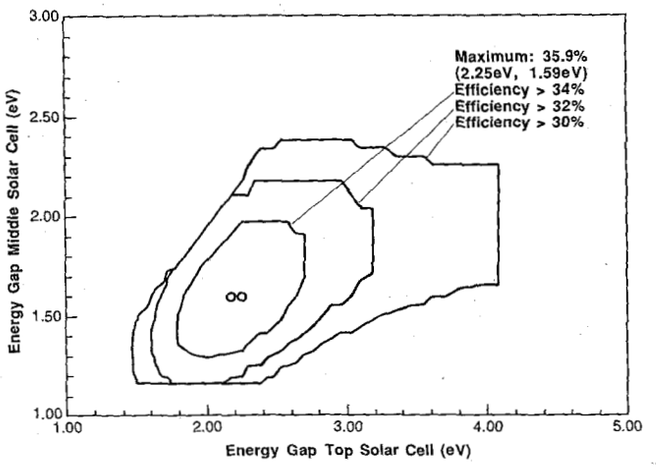

Fig. 9. Three-solar-cell tandem system efficiencies including losses with a silicon bottom solar cell for the spectrum *AM1.5* global.

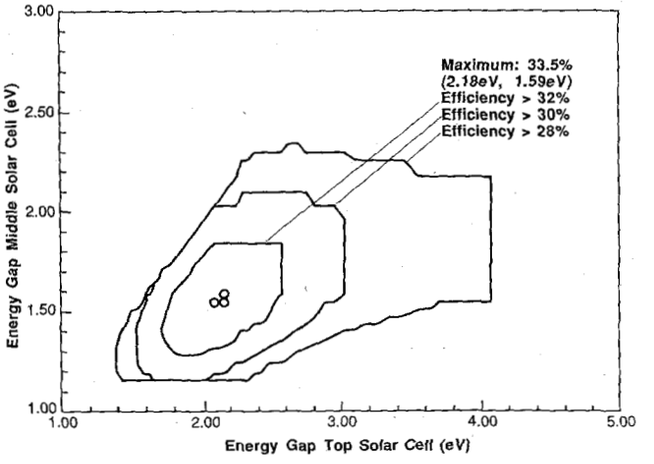

Fig. 10. Three-solar-cell tandem system efficiencies including losses with a silicon bottom solar cell for the spectrum *AM1.5* direct.

solar cell there are 14.0- and 2.0-percent, for the bottom solar cell 18.0- and 2.0-percent optical and electrical losses. As a result we can state that with the losses in J_{sc} the efficiency of an optimal two-solar-cell four-terminal tandem configuration will be over 30 percent for each spectrum (see Fig. 8).

VIII. Three-Solar-Cell Tandem Systems

At present two-solar-cell tandem systems are being developed and the results are promising [32]. Three-solar-cell tandem structures have not been given much attention because the increase in efficiency by the third solar cell is modest with a substantial increase in complexity of fabrication [8]. But as the development proceeds, the demand for ultrahigh-efficiency solar cells will arise. Efficiencies far over 30 percent will be the goal because calculations including realistic losses show that it is possible to reach 30-percent efficiency with a two-solar-cell tandem structure.

Table II shows the maximum-efficiency combination for a three-solar-cell tandem system for the standard spectra. There are a variety of materials available, particularly III–V semiconductors, to build that device. Figs. 9, 10, and 11 show three-solar-cell six-terminal tandem system efficiencies including losses for a structure with a silicon bottom solar cell. The dashed line in Fig. 11 shows the cutoff, above which no tandem solar-cell bandgap combination is possible because (12) is violated.

$$E_{g\text{top}} > E_{g\text{bottom}}. \tag{12}$$

IX. Tandem Solar-Cell Performance Limits

If two, three, or more solar cells are put in tandem to yield higher maximum efficiencies, it is useful to know the performance limits based on the spectral p–n junction model. The lower limit, a single-junction solar cell, has been discussed earlier. The upper limit will be given by the largest number of solar cells stacked to one tandem system. In this case a maximum of the incident solar energy can be converted because there is no loss of subbandgap photons, which are transmitted, and of high-energy photons, which after creating only one electron–hole pair dissipate their excess energy in the form of heat. This value is given by the number of data points that represent the incident spectrum. Every spectral element of the irradiance curve can be assigned to one solar cell to generate electricity. The highest efficiency is the sum of the maximum power of all solar cells normalized by the total incident power. It is expected that the maximum efficiency is very high. But as the number of solar cells in the structure increases, less available energy is converted due to losses in the fill factor, which drops to the value of 0.25.

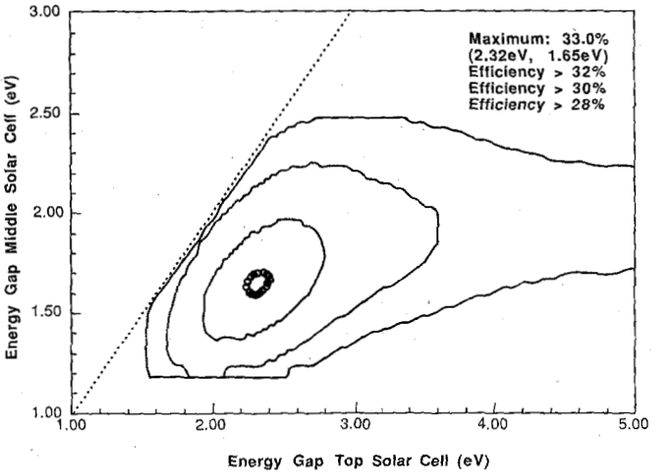

Fig. 11. Three-solar-cell tandem system efficiencies including losses with a silicon bottom solar cell for the spectrum *AM0*.

Fig. 12 shows the maximum system efficiency of a tandem configuration dependent on the logarithm of the number of solar cells in the structure. On a linear plot it can be seen that the efficiency rises fast with the number of solar cells and continues with a small slope. This behavior leads to the conclusion that a much smaller number of solar cells than the amount of data points can yield almost

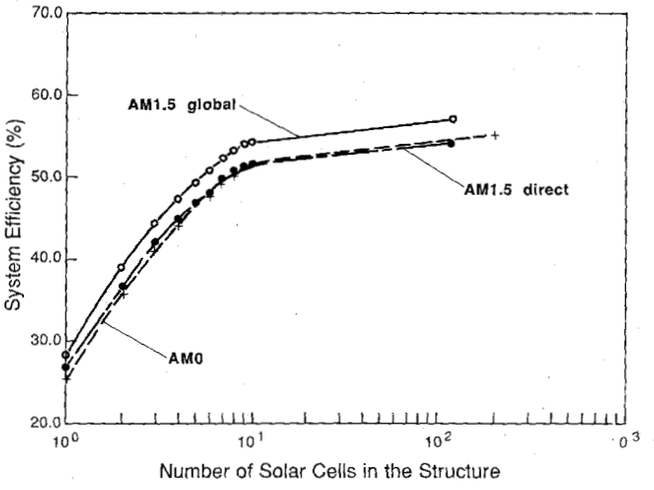

Fig. 12. Maximum tandem system efficiencies dependent on the number of solar cells in the configuration for the standard spectra.

the maximum efficiency. For *AM*1.5 global a system with 10 solar cells in tandem will yield efficiencies of 54.4 percent, 94.9 percent of the maximum possible.

X. The Increase In Efficiency Under Concentration

Besides the advantage of a small-size solar cell, the concentrator configuration offers a higher efficiency compared to unconcentrated operation. For an evaluation of the system performance the relative increase of the efficiency with the concentration ratio has to be known. With valid assumptions the relationship can be derived analytically.

To calculate the efficiency under concentration, the maximum power point, which is given as a function of J_{sc}, J_0, and T by (10) and (11), has to be found. The transcendental equation (11) for the voltage of the maximum power point cannot be solved explicitly. But with assumption (13)

$$\ln\left(1 + \frac{e \cdot V_m}{k \cdot T}\right) \approx \text{const.} = a \tag{13}$$

the voltage V_m of the maximum power point can be written down (see (14)). For most applications the voltage of the maximum power point is between 0.3 and 1.8 V. This corresponds to values for a from 2.5 to 4.3. Therefore $a = 3.4$ can be considered a good average value.

$$V_m = \frac{kT}{e} \cdot \left(\ln\left(\frac{J_{sc}}{J_0} + 1\right) - a\right). \tag{14}$$

With the fact that

$$J_{sc} \gg J_0 \tag{15}$$

for energy gaps larger than 0.7 eV further abbreviations can be made. Accordingly the maximum power point can be represented by (16).

$$P_m = J_{sc} \cdot (e^{-a} - 1) \cdot \frac{kT}{e} \cdot \left(\ln\frac{J_{sc}}{J_0} - a\right). \tag{16}$$

Under concentration X the short-circuit current density will increase to $X \cdot J_{sc}$. With the maximum power under concentration X, $P_m(X)$, and the total incident solar power, unconcentrated P_s and concentrated $X \cdot P_s$, the efficiency $\eta(X)$ can be calculated as a function of the concentration.

To determine the increase in efficiency under concentration the relative change of the efficiency at the concentration ratio X is calculated

$$\frac{\eta(X) - \eta(1)}{\eta(1)} = \frac{P_m(X)}{X \cdot P_s} \cdot \frac{P_s}{P_m(1)} - 1 \tag{17}$$

$$= \frac{1}{X} \cdot \frac{X \cdot J_{sc} \cdot (e^{-a} - 1) \cdot \frac{kT}{e} \cdot \left(\ln\frac{X \cdot J_{sc}}{J_0} - a\right)}{J_{sc} \cdot (e^{-a} - 1) \cdot \frac{kT}{e} \cdot \left(\ln\frac{J_{sc}}{J_0} - a\right)} - 1 \tag{18}$$

$$= \frac{\ln\frac{X \cdot J_{sc}}{J_0} - a}{\ln\frac{J_{sc}}{J_0} - a} - 1 \tag{19}$$

$$= \frac{1}{\ln\frac{J_{sc}}{J_0} - a} \cdot \ln X. \tag{20}$$

The result (see (20)) shows a linear increase of the efficiency ratio with ln (X) or a logarithmic growth of the concentrated—unconcentrated efficiency relation with the concentration X.

XI. Conclusions

Tandem solar cells have higher theoretical efficiencies than single-junction solar cells. A consistent expression for the reverse-saturation current density using an adjustable constant C was developed. This expression is based on a fit to experimentally achieved open-circuit voltages. With the spectral p–n junction model the efficiencies of solar cells in tandem configurations are calculated. The generated data were used to determine the highest efficiency bandgap combination. Including realistic losses for a two-solar-cell tandem system with a Si solar cell on the bottom, the optimum bandgap for the top cell has been determined.

Increased efficiency can be obtained from a three-solar-cell six-terminal tandem configuration. The plots for maximum efficiency for two solar cells on top of a Si bottom solar cell are shown. Still higher efficiencies can be achieved with more solar cells in the tandem system. Ten solar cells in a tandem system will yield 94.9 percent of

the highest possible efficiency, 57.3 percent ($AM1.5$ global).

The efficiency of a solar cell increases with the concentration ratio X. The derived expression for the relative increase in efficiency under concentration shows a linear behavior with ln (X).

Acknowledgment

The authors would like to thank J. B. McNeely for helpful discussions.

References

[1] D. Trivich and P. A. Flinn, "Maximum efficiency of solar energy conversion by quantum processes," in *Solar Energy Research*, F. Daniels, J. A. Duffie, Eds. Madison, WI: Univ. of Wisconsin Press, 1955, p. 143.

[2] E. D. Jackson, "Areas for improvement of the semiconductor solar energy converter," in *Trans. Intern. Conf. Use of Solar Energy—The Scientific Basis*, vol. V, p. 122, 1955.

[3] J. J. Loferski, "Theoretical and experimental studies of tandem or cascade solar cells: A review," in *Conf. Rec. 16th IEEE Photovoltaic Specialists Conf.*, pp. 648–654, 1982.

[4] K. W. Mitchell, "High efficiency concentrator solar cells," in *Conf. Rec. 15th IEEE Photovoltaic Specialists Conf.*, pp. 142–146, 1981.

[5] J. A. Hutchby, R. J. Markunas, M. L. Timmons, P. K. Chiang, and S. M. Bedair, "A review of multijunction concentrator solar cells," in *Conf. Rec. 18th IEEE Photovoltaic Specialists Conf.*, pp. 20–27, 1985.

[6] M. F. Lamorte and D. H. Abbott, "Computer modeling of a two-junction, monolithic cascade solar cell," *IEEE Trans. Electron Devices*, vol. ED-27, pp. 231–249, Jan. 1980.

[7] ——, "Cascade solar cells design for high temperature operation," *IEEE Trans. Electron Devices*, vol. ED-27, pp. 831–840, Apr. 1980.

[8] J. C. C. Fan, B. Y. Tsaur, and B. J. Palm, "Optimal design of high-efficiency tandem cells," in *Conf. Rec. 16th IEEE Photovoltaic Specialists Conf.*, pp. 692–701, 1982.

[9] H. Pauwels and A. De Vos, "Determination of the maximum-efficiency solar-cell structure," *Solid-State Electron.*, vol. 24, pp. 835–843, Sept. 1981.

[10] C. Riordan, T. Cannon, D. Myers, and R. Bird, "Solar irradiance models, data, and instrumentation for PV device performance analysis," in *Conf. Rec. 18th IEEE Photovoltaic Specialists Conf.*, pp. 957–962, 1985.

[11] R. L. Moon, L. W. James, H. A. Vander Plas, T. O. Yep, G. A. Antypas, and Y. Chai, "Multigap solar-cell requirements and the performance of AlGaAs and Si cells in concentrated sunlight," in *Conf. Rec. 13th IEEE Photovoltaic Specialists Conf.*, pp. 859–867, 1978.

[12] R. A. LaRue, P. G. Borden, M. J. Ludowise, P. E. Gregory, and W. T. Dietze, "The metal interconnected cascade solar cell," in *Conf. Rec. 16th IEEE Photovoltaic Specialists Conf.*, pp. 228–230, 1982.

[13] M. Wolf, "A new look at silicon solar-cell performance," *Energy Conversion*, vol. 11, pp. 63–73, June 1971.

[14] S. Sakai and M. Umeno, "Theoretical analysis of new wavelength-division solar cells," *J. Appl. Phys.*, vol. 51, pp. 5018–5024, Sept. 1980.

[15] L. M. Fraas, B. K. Shin, J. A. Cape, R. A. Ransom, and D. E. Sawyer, "Ternary III–V solar cells for multicolor applications," in *Conf. Rec. 16th IEEE Photovoltaic Specialists Conf.*, pp. 655–662, 1982.

[16] R. Matson, R. Bird, and K. Emery, "Terrestrial solar spectra, solar simulation, and solar-cell efficiency measurement," Solar Energy Research Institute, SERI/TR-612-964, Sept. 1981.

[17] C. Riordan, Solar Energy Research Institute, Golden, CO, private communication.

[18] M. P. Thekaekara, "Extraterrestrial solar spectrum, 3000–6000 Å at 1Å intervals," *Appl. Opt.*, vol. 13, pp. 518–522, Mar. 1974.

[19] C. Hu and R. M. White, *Solar Cells*. New York: McGraw-Hill, 1983, p. 21.

[20] W. Shockley, "The theory of p–n junctions in semiconductors and p–n junction transistors," *Bell Syst. Tech. J.*, vol. 28, pp. 435–489, July 1949.

[21] M. A. Green, *Solar Cells*. Englewood Cliffs, NJ: Prentice-Hall, 1982, p. 88.

[22] J. J. Loferski, "Theoretical considerations governing the choice of the optimum semiconductor for photovoltaic solar energy conversion," *J. Appl. Phys.*, vol. 27, pp. 777–784, July 1956.

[23] M. A. Green, A. W. Blakers, Shi Jiqun, E. M. Keller, S. R. Wenham, R. B. Godfrey, T. Szpitalak, and M. R. Willison, "Towards a 20-percent efficient silicon solar cell," in *Conf. Rec. 17th IEEE Photovoltaic Specialists Conf.*, pp. 386–389, 1984.

[24] R. P. Gale, "High-efficiency single-crystal solar cells," in *Proc. SERI Photovoltaic Advanced Research and Development Project, 6th Annual Review Meeting* (Golden, CO, 1984), SERI/CP-211-2507, pp. 105–106.

[25] W. Shockley and H. J. Queisser, "Detailed balance limit of efficiency of p–n junction solar cells," *J. Appl. Phys.*, vol. 32, pp. 510–519, Mar. 1961.

[26] M. B. Prince, "Silicon solar energy converters," *J. Appl. Phys.*, vol. 26, pp. 534–540, May 1955.

[27] M. E. Nell and A. M. Barnett, "A $GaAs_{1-x}P_x$ top tandem solar cell with high performance," in *Proc. 6th E.C. European Photovoltaic Solar Energy Conf.*, pp. 265–269, 1985.

[28] M. E. Nell and A. M. Barnett, "$GaAs_{1-x}P_x$ high-efficiency tandem solar cells," in *Conf. Rec. 18th IEEE Photovoltaic Specialists Conf.*, pp. 116–121, 1985.

[29] A. M. Barnett, M. G. Mauk, J. C. Zolper, I. W. Hall, W. A. Tiller, R. B. Hall and J. B. McNeely, "Thin-film silicon and GaAs solar cells," in *Conf. Rec. 17th IEEE Photovoltaic Specialists Conf.*, pp. 747–754, 1984.

[30] J. M. Gee, "Mechanically-stacked multijunction solar cells," in *Proc. 6th E.C. European Photovoltaic Solar Energy Conf.*, pp. 245–253, 1985.

[31] J. B. McNeely, G. H. Negley, M. E. Nell, S. Brennan, and A. M. Barnett, "Design and fabrication of GaAsP silicon tandem solar cell," in *Conf. Rec. 18th IEEE Photovoltaic Specialists Conf.*, pp. 151–156, 1985.

[32] L. M. Fraas, J. A. Cape, P. S. McLeod, and L. D. Partain, "High efficiency $GaAs_{0.7}P_{0.3}$ solar cell on a transparent GaP wafer," *J. Appl. Phys.*, vol. 57, pp. 2302–2304, Mar. 1985.

*

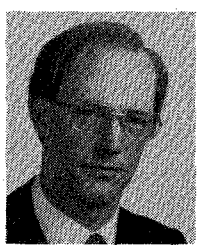

Matthias E. Nell (S'84–M'85) was born in Stade/Elbe, Germany, on April 1, 1956. He received the Dipl.-Phys. degree from the Technical University of Aachen, Germany, in 1983, and the M.E.E. degree from the University of Delaware, Newark, in 1985.

His research interest is in optics and semiconductor physics. From 1981 to 1983, he worked on models and measurement techniques for the infrared spectroscopy of powders, and from 1983 to 1985, on the design and preparation of ternary III–V semiconductor solar cells. In 1985, he joined the Institute for Electronic Materials of the Technical University of Berlin, Germany. His present work concentrates on LPE preparation and model calculations for device design and analysis of AlGaAs solar cells.

Mr. Nell is a member of Eta Kappa Nu and the German Physical Society.

*

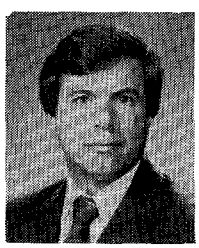

Allen M. Barnett (S'64–M'66–SM'79) was born in Oklahoma City, OK. He received the B.S.E.E. and M.S. degrees from the University of Illinois, Urbana, in 1962 and 1963, respectively. He received the Ph.D. degree in electrical engineering from the Carnegie Institute of Technology, Pittsburgh, PA, in 1966.

He has been Professor of Electrical Engineering at the University of Delaware, Newark, since 1976. He was also Director of the Institute of Energy Conversion at the University of Delaware

from 1976 to September 1979. He has been a consultant to the Astropower Division of Astrosystems, Inc. since 1983. He was president of Xciton Corporation from 1972 to 1975 and worked for the General Electric Company at the Electronics Laboratory and the Research and Development Center from 1966 to 1971. He is developing advanced semiconductor devices based on the hetero-epitaxial growth of semiconductors on silicon, III–V, and noncrystalline substrates. These devices include thin-film polycrystalline silicon, thin-film gallium arsenide, and other III–V compound solar cells. He is also developing hybrid silicon/GaAs optically interconnected circuits.